A STREAMTUBE APPROXIMATION FOR CALCULATION OF REACTION RATES IN THE INVISCID FLOW FIELD OF HYPERSONIC OBJECTS

S. C. Lin and J. D. Teare
Avco-Everett Research Laboratory
Everett 49, Massachusetts

Abstract

An approximate method for calculating the chemical reactions and ionization rates in the inviscid flow field around hypersonic objects of arbitrary shape is proposed. This method essentially consists of an iterative scheme in which the chemical reactions along individual streamtubes are followed in a pre-determined pressure field. Preliminary numerical results will be presented to illustrate the degree of departure from thermodynamic equilibrium for the various chemical reactions along a typical streamtube to be expected under different flight conditions.

Introduction

Inclusion of finite reaction rates in hypersonic flow field calculations is generally complicated by the fact that the equation of state for the gas has now become an explicit function of time, so that the usual Eulerian description of the flow becomes inadequate. For the supersonic region the well known method of characteristics has been adapted (1 - 3) to deal with flows of reacting gases, but the actual numerical method becomes rather unwieldy and is susceptible to the usual problem of accumulative error, the magnitude of which is difficult to assess.

An alternative approach to this problem is to divide the inviscid flow field into a number of co-axial streamtubes according to the strength (i.e., obliqueness) of the bow shock wave through which the streamtube passes. By treating the different streamtubes as separate entities in a pre-determined pressure field, the temperature, density, and chemical compositions of the gas can be determined as functions of distance behind the bow shock wave along the streamtube by integrating the chemical rate equations subject to the constraints of the conservation laws. The ionization history along the streamtube

can likewise be calculated by integrating the corresponding rate equations according to the local temperature and chemical species histories just determined.

The Pressure-Field Iteration Method

To specify the pressure field for the streamtube calculation, the following iterative scheme is proposed.

In the first approximation, the pressure distribution in the hypersonic flow field may be obtained from any one of the existing methods (4). For flow situations in which the chemistry should be near equilibrium, it is reasonable to take a pressure distribution obtained from an equilibrium flow field calculation. At the other extreme, where very little chemistry will take place in the flow field, it is equally reasonable to obtain a pressure distribution from a "frozen flow" calculation. For some classes of body it is clearly possible to obtain substantial differences between the equilibrium and frozen flow pressure distributions. This is especially true for bodies with a sharp corner and sudden Prandtl-Meyer expansion. However, for blunt nosed bodies in which the expansion takes place more gradually it is not expected that the pressure distribution will be very sensitive to the state of the chemistry in the gas.

When the pressure distributions have been chosen, the density and flow velocity distributions for the chemically reacting gas can be determined by the method described above, and the cross sectional area along each streamtube can be determined. Then, working from the innermost streamtube (i.e., the streamtube that passes through the normal shock near the stagnation point) outward, the outer boundary for the last chemically active streamtube can be determined. Treating this boundary as a solid boundary, the pressure distribution in the hypersonic flow field can now be re-calculated according to the standard method (since the non-reacting gas assumption will be perfectly valid beyond such a boundary). The resultant pressure distribution can then be used to start the second approximation.

The iterative scheme proposed above takes advantage of the fact that chemical reactions can only occur within the high entropy regions of the hypersonic flow field (i.e., streamtubes that have passed through the strong portion of the bow shock wave). Since the volume occupied by the high entropy region is generally small compared with the total volume of the flow field, it is clear that the overall pressure distribution will not be very sensitive to the thermodynamic state of the gas

within the high entropy region*. As a result, one may expect rapid convergence of this iterative process even in the presence of considerable error in the initial pressure specification.

It may be mentioned that even though we have only been concerned with the inviscid flow field so far, this pressure-field iteration method can also be extended to treat the reaction rate problem in the viscous part of the flow field as well. The fundamental point to be made is that the pressure disturbances generally propagate much faster than the viscous effects, so that a fairly clean separation of the entire hypersonic flow field into two distinct parts is generally possible. That is: an inner part containing all the chemically reacting gas and viscous effects which play only a minor role in determining the overall pressure distribution in the flow field; and an outer part which contains no significant chemical reaction, but controls the overall pressure distribution through the decay history of the bow shock wave.

Integration of the Chemical Rate Equations Along the Streamtube

Integration of the chemical rate equations along the streamtube can be done by a natural extension of the earlier methods that have been developed for reaction profile calculations behind normal shock waves (5, 6). Some detailed descriptions of these methods can be found in (7, 8, and 9).

For the case of normal shock waves, the chemical rate equations

$$\frac{dX_i}{dt} = F_i(T, \rho, X_1, X_2, \ldots X_i \ldots) \qquad (1)$$

governing the relative concentration, X_i, of each of the chemical species are integrated under the constraints of the Bethe-Teller equations for conservation of energy, mass, and momentum. X_i is most conveniently expressed in units of moles per mole of unshocked gas. Rate equations describing the vibrational excitation of the O_2 and N_2 molecules are also integrated under the same conservation constraints.

In the present case, where integration of the rate equations is to be carried out along streamtubes, the cross-sectional

*It may be noted that the argument of small volume does not apply to the stagnation region, which is mostly at high entropy. However, since the Newtonian approximation is generally valid within this region, the insensitivity of pressure to the thermodynamic state of the gas still holds.

areas of which are yet unknown, the energy equation,

$$H + \frac{u^2}{2} = \text{constant} \tag{2}$$

remains unchanged, but the algebraic mass and momentum equations must be replaced by,

$$\rho u \frac{du}{dx} = -\left(\frac{dp}{dx}\right)_o \tag{3}$$

$$dt = \frac{dx}{u} \tag{4}$$

where x denotes the streamwise distance along the streamtube; u is the streamwise velocity, and $\left(\frac{dp}{dx}\right)_o$ is the local pressure gradient as given by the pre-determined pressure distribution.

The specific enthalpy H and the gas density ρ are, of course, functions of temperature, chemical composition and vibrational excitation as before. That is,

$$H = H\left(T, \epsilon_{VO_2}, \epsilon_{VN_2}, X_1, X_2, \ldots X_i \ldots\right) \tag{5}$$

where ϵ_V is the average vibrational energy of the molecules at time t, and

$$\rho/\rho_o = pT_o/p_oT \sum_i X_i \tag{6}$$

Equations (1) through (6) form a complete system of equations sufficient to determine all the state variables as functions of streamwise distance behind the bow shock wave. This formulation is basically similar to the one-dimensional analyses reported independently by Bloom and co-workers (10, 11).

The specific chemical reaction and ionization rate constants employed in the present numerical examples are summarized in Tables 1 and 2. Some discussions concerning the sources and uncertainties of these rate constants can be found in (12 and 13). A more recent tabulation, with a fuller discussion, can be found in (14).

Numerical Examples for the Case of a Hemisphere-Cylinder

Preliminary calculations of the chemical reaction and ionization histories along some typical streamtubes have been made for the case of a hemisphere cylinder of 1 ft radius at a free-stream velocity of 18,000 ft/sec and at three different densities corresponding to flight altitudes of 250,000, 150,000

Table 1. Rate Constants for Chemical Processes

Reaction	Catalyst M	Rate Constant
$O_2 + M + 5.1\,ev \underset{k_R}{\overset{k_D}{\rightleftharpoons}} O + O + M$	Ar, N, N_2, NO	$k_D = \frac{3.6 \times 10^{18}}{T} \exp(-59373/T)\,cm^3/mole\,sec$
	O_2	$k_D = \frac{1.2 \times 10^{23}}{T^2} \exp(-59373/T)\,cm^3/mole\,sec$
	O	$k_D = \frac{3.2 \times 10^{23}}{T^2} \exp(-59373/T)\,cm^3/mole\,sec$
$N_2 + M + 9.8\,ev \underset{k_R}{\overset{k_D}{\rightleftharpoons}} N + N + M$	Ar, O, O_2, NO	$k_R = 5 \times 10^{19} \times T^{-1.5}\,cm^6/mole^2 sec$
	N_2	$k_R = 1.5 \times 10^{20} \times T^{-1.5}\,cm^6/mole^2 sec$
	N	$k_R = 7.5 \times 10^{20} \times T^{-1.5}\,cm^6/mole^2 sec$
$NO + M + 6.5\,ev \underset{k_R}{\overset{k_D}{\rightleftharpoons}} N + O + M$	O, O_2, N N_2, NO	$k_R = 8.6 \times 10^{20} \times T^{-1.5}\,cm^6/mole^2 sec$
$NO + O + 1.4\,ev \underset{k_2}{\overset{k_1}{\rightleftharpoons}} O_2 + N$		$k_2 = 1 \times 10^{12} T^{0.5} \exp(-3120/T)\,cm^3/mole\,sec$
$N_2 + O + 3.3\,ev \underset{k_2}{\overset{k_1}{\rightleftharpoons}} NO + N$		$k_2 = 1.3 \times 10^{13}\,cm^3/mole\,sec$
$N_2 + O_2 + 1.9\,ev \underset{k_2}{\overset{k_1}{\rightleftharpoons}} NO + NO$		$k_2 = 2.6 \times 10^{23} \times T^{-2.5} \exp(-43030/T)\,cm^3/mole\,sec$

Note: These rate constants were used in the calculations shown in Figs. 2 through 6. For an updated tabulation the interested reader is referred to Ref. 14. The recent revisions do not materially affect the results of the present flow field calculations.

Table 2. Electronic Processes

No.	Reaction	Exothermic Rate Constant cm^3/sec
i	$N + O + 2.8\ ev \rightleftarrows NO^+ + e$	$3 \times 10^{-3}\ T^{-3/2}$
ii	$N^* + N + (5.8\ ev) \rightleftarrows N_2^+ + e$	$1.6 \times 10^{-2}\ T^{-3/2}$
iii	$O^* + O + (6.9\ ev) \rightleftarrows O_2^+ + e$	$3.2 \times 10^{-3}\ T^{-3/2}$
iv	$O_2^+ + O + 1.6\ ev \rightleftarrows O_2 + O^+$	$1.3 \times 10^{-12} T^{1/2}$
v	$N^+ + N_2 + 1.0\ ev \rightleftarrows N + N_2^+$	$1.3 \times 10^{-12} T^{1/2}$

For reactions (ii) and (iii), the asterisks indicate that the products of dissociative recombination may be in excited states. The energies in parentheses are appropriate when both atoms are in the ground state.

and 100,000 ft respectively. The geometrical configuration depicting the approximate location of three different streamlines near the bow shock wave is illustrated in Fig. 1. The translational temperatures immediately behind the bow shock (i.e., before vibrational relaxation and dissociation take place) are approximately as follows:

Streamline	Starting Temperature
	°K
A	14,500
B	11,700
C	6,750

The pressure distribution employed in the first approximation along streamline A is illustrated in Fig. 2, which also shows the corresponding density distribution computed both by means of the present method (solid curve) and by means of the usual equilibrium isentropic expansion from the stagnation region (dashed curve). This particular pressure distribution was based on a smooth joining of the uncorrected Newtonian pressure distribution in the stagnation region and the pressure distribution at large distances from the stagnation point as obtained from the second-order blast wave theory (15, 16). It is in good agreement with the pressure distribution obtained from method of characteristics calculations for equilibrium flow at this flight condition.

The resultant temperature, chemical species, and electron concentrations along streamline A as calculated from the first approximation are illustrated in Figs. 3 through 6 (solid curves) for comparison with the corresponding quantities calculated for the equilibrium isentropic expansion (dashed curves).

Discussion

From the preliminary results shown in Figs. 3 through 6, it is clear that the finite reaction rates can be expected to play very dominant roles in determining the translational temperature and chemical composition histories in the high entropy region of a hypersonic object, even at relatively low flight altitudes. Generally speaking, the overall effect of the finite reaction rates is to depress the concentration of active species in the compression region (upstream of the sonic point), and to enhance the concentrations of these species in the expansion region (downstream of the sonic point) when

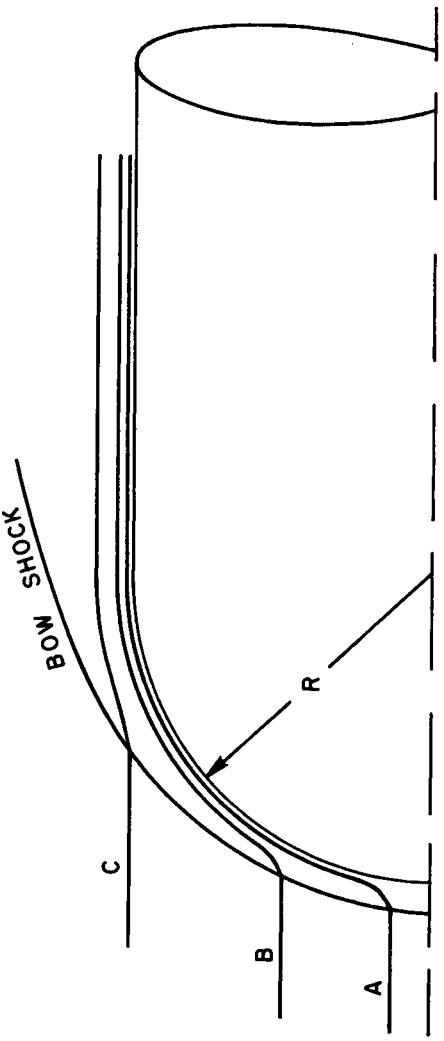

Fig. 1. Streamtubes Computed for Hemisphere-Cylinder, R = 1 ft = 30.48 cm.

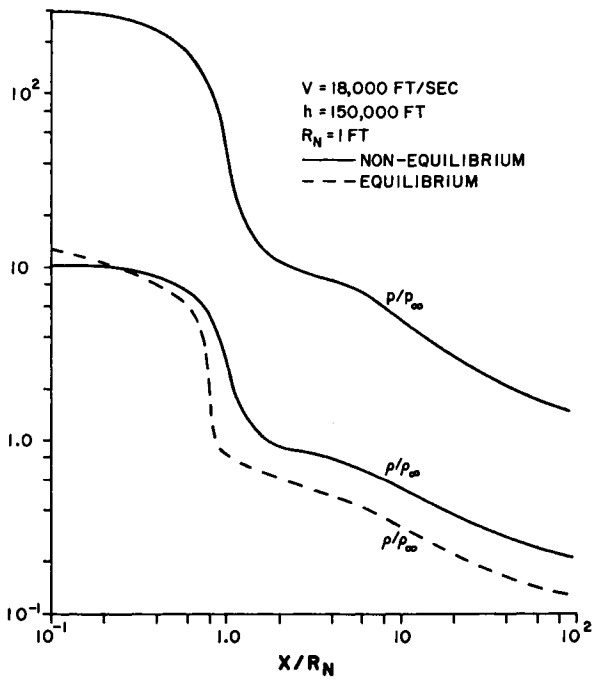

Fig. 2. Hemisphere-Cylinder Flow Field. Pressure and Density Distributions Along Streamtube A at 150,000-Foot Altitude.

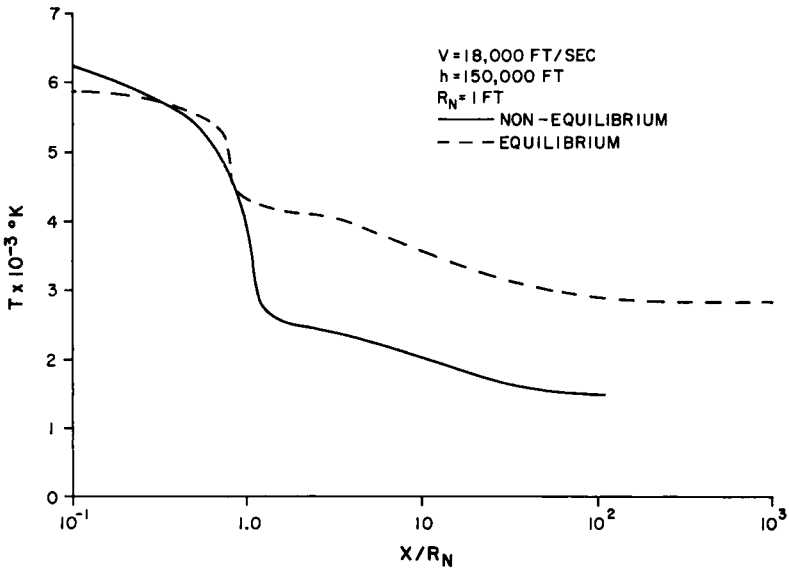

Fig. 3. Hemisphere-Cylinder Flow Field. Temperature Distribution Along Streamtube A at 150,000-Foot Altitude.

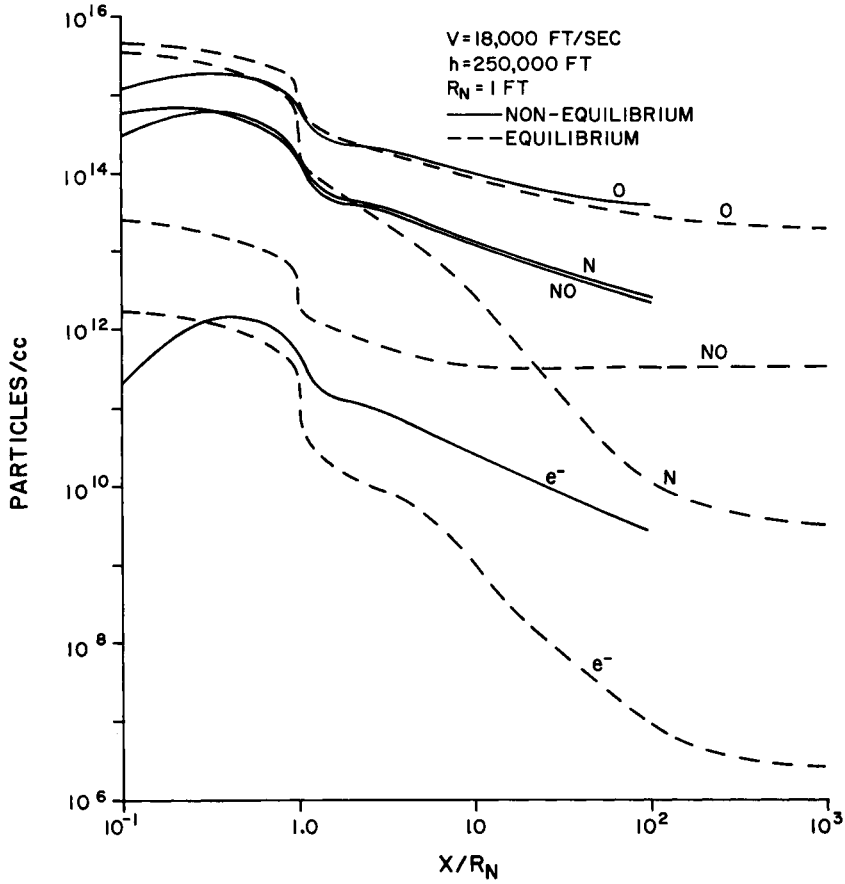

Fig. 4. Hemisphere-Cylinder Flow Field. Particle Concentrations Along Streamtube A at 250,000-Foot Altitude.

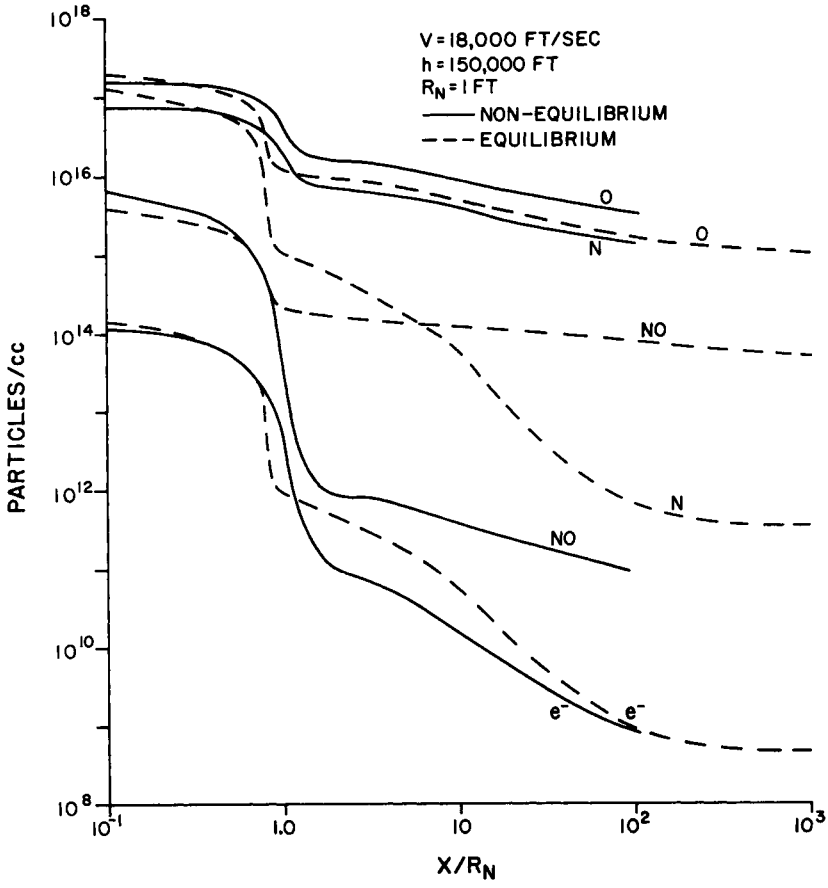

Fig. 5. Hemisphere-Cylinder Flow Field. Particle Concentrations Along Streamtube A at 150,000-Foot Altitude.

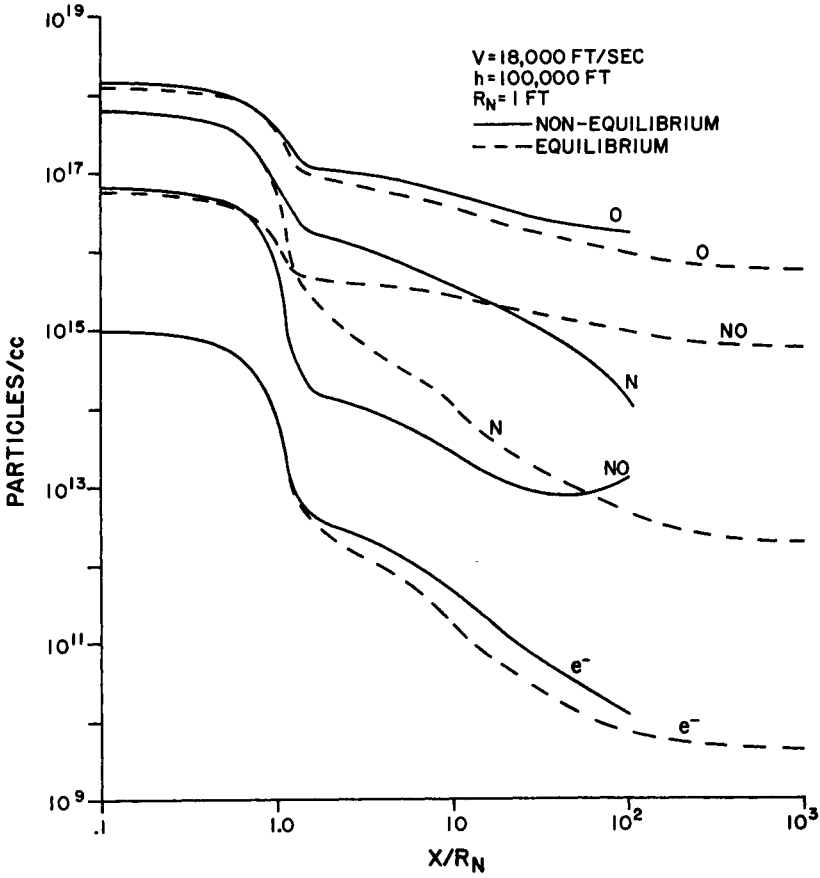

Fig. 6. Hemisphere-Cylinder Flow Field. Particle Concentrations Along Streamtube A at 100,000-Foot Altitude.

compared with the reference concentrations based on the quasi-equilibrium flow assumption, and that the degree of departure from the reference concentration is generally much more marked in the latter region. One exception to the above statement, however, is the concentration of nitric oxide, which shows just the opposite trend on account of the rapid "shuffle reactions" leading to the NO formation and destruction processes.

In regard to the ionization history, it is interesting to note that while the electron concentration in the compression region generally follows the ambient air density with changing altitude (i.e., approximately constant degree of ionization), the absolute electron concentration tends to remain constant at large distances from the stagnation point in the expansion region (e.g., at $x/R_N = 100$, $10^9 \lesssim n \lesssim 10^{10}$ cm^{-3} for $250,000 \geq h \geq 100,000$ ft). This is due to the fact that the translational temperature remains so low that the electron concentration becomes self-limiting according to the dissociative recombination process*,

$$e + NO^+ \rightarrow N + O$$

Thus, in the fully expanded region

$$\frac{dn_e}{dt} \approx -\alpha n_e^2, \tag{8}$$

where $\alpha \approx 3 \times 10^{-3} T^{-3/2}$ cm^3/sec from Table 2. By integration of Eq. (8), one obtains

$$\frac{1}{(n_e)_2} - \frac{1}{(n_e)_1} = \alpha \Delta t$$

or

$$\frac{1}{(n_e)_2} = \frac{1}{(n_e)_1} + \frac{3 \times 10^{-3} \bar{T}^{-3/2} x_{12}}{\bar{u}}$$

where $(n_e)_2$ and $(n_e)_1$ are the electron concentrations at points separated by a distance x_{12} along a streamtube, and $\bar{T}$, $\bar{u}$ are the mean temperature and flow velocity respectively in this portion of the streamtube. For $(n_e)_1 >> (n_e)_2$, this yields $(n_e)_2 \approx 300 \bar{T}^{-3/2} \bar{u}/x_{12} \propto 1/x_{12}$.

*It may be pointed out that the apparent resemblance between the "non-equilibrium" and the "equilibrium" electron concentrations in Figs. 5 and 6 is purely accidental, and definitely does not mean that the electron concentration is in quasi-equilibrium with the flow field.

References

1. Chu, B. T., "Wave Propagation and the Method of Characteristics in Reacting Gas Mixtures with Application to Hypersonic Flow," Brown University Report WADC TN-57-213, May 1957, ASTIA Doc. No. AD 118350.

2. Wood, W. W., and Kirkwood, J. G., J. Appl. Phys., vol. 28, 1957, p. 395.

3. Lin, C. C., Quart. Appl. Math., vol. VII, 1950, p. 443.

4. Hayes, W. D., and Probstein, R. F., Hypersonic Flow Theory, Academic Press, New York and London, 1959.

5. Duff, R. E., and Davidson, N., Bull. Am. Phys. Soc., Ser. II, vol. 4, 1959, p. 195.

6. Lin, S. C., and Teare, J. D., Bull. Am. Phys. Soc., Ser. II, vol. 4, 1959, p. 195.

7. Duff, R. E., and Davidson, N., J. Chem. Phys., vol. 31, 1959, p. 1018.

8. Hammerling, P., Teare, J. D., and Kivel, B., Phys. of Fluids, vol. 2, 1959, p. 422.

9. Wray, K., and Teare, J. D., "A Shock Tube Study of the Kinetics of Nitric Oxide at High Temperatures," Avco-Everett Research Laboratory, Research Report 95, 1961.

10. Bloom, M. H., and Steiger, M. H., J. Aero. Sci., vol. 27, 1961, p. 821.

11. Vaglio-Laurin, R., and Bloom, M. H., ARS Preprint No. 1976-61.

12. Wray, K., Teare, J. D., Kivel, B., and Hammerling, P., "Relaxation Processes and Reaction Rates Behind Shock Fronts in Air and Component Gases," Avco-Everett Research Laboratory, Research Report 83, 1959.

13. Lin, S. C., and Fyfe, W. I., Phys. of Fluids, vol. 4, 1961, p. 238.

14. Wray, K., "Chemical Kinetics of High Temperature Air," Avco-Everett Research Laboratory, Research Report 104, 1961. ARS Preprint No. 1975-61.

15. Lees, L., and Kubota, T., J. Aero. Sciences, vol. 24, 1957, p. 195.

16. Feldman, S., "A Numerical Comparison Between Exact and Approximate Theories of Hypersonic Inviscid Flow Past Slender Blunt-nosed Bodies," Avco-Everett Research Laboratory, Research Report 71, 1959, ASTIA Doc. No. AD 226-728.